Some aspects regarding the influence of the anisotropy of an AA2021-T351 rolled thick plate on its tribological behaviour

E. PIRVA[a], A. TUDOR[b], A. GAVRUS[c*], N. STOICA[d], S. CANANAU[e]

a. PhD Int. Thesis UPB-INSA Rennes, University Politehnica of Bucharest (UPB), 313 Splaiul Independentei, 060042 Bucharest, Romania, email: elisabeta.pirva@yahoo.com
b. Prof. University Politehnica of Bucharest (UPB), OMT Department, 313 Splaiul Independentei, 060042 Bucharest, Romania, email: andreitudor1947@gmail.com
c. Assoc. Prof. University Brittany Loire (UBL), INSA Rennes, LGCGM (EA 3913), 20 av. des Buttes de Coesmes, 35708 Rennes, France, email : adinel.gavrus@insa-rennes.fr
d. Assistant Prof. University Politehnica of Bucharest (UPB), OMT Department, 313 Splaiul Independentei, 060042 Bucharest, Romania, email: nicolae.stoica@upb.ro
e. Prof. University Politehnica of Bucharest (UPB), OMT Department, 313 Splaiul Independentei, 060042 Bucharest, Romania, email: s_cananau@yahoo.com

Résumé:

Cette étude scientifique vise à étudier l'influence de l'anisotropie d'une plaque épaisse laminée en alliage d'aluminium AA2024-T351 sur les propriétés tribologiques en surface, à partir d'études antérieures expérimentales et numériques concernant le comportement mécanique en volume et en surface. Des essais tribologiques ont était réalisés sur un échantillon de 10 mm d'épaisseur avec un disque en polyéthylène de masse moléculaire très élevée (UHMWPE). Le test tribométrique utilisé implique la génération d'un mouvement à l'échelle locale le long des trajectoires spécifiques à différents orientations sous l'action d'une force normale constante et une vitesse de glissement constante. Tous les tests ont été faites avec trois forces normales différentes (3N, 5N, 7N) est cinq vitesses de translation (0.005 mm/s, 0.05 mm/s, 0.5 mm/s, 1mm/s and 5mm/s) sur une distance d'environ 3 mm. Afin d'analyser l'influence de l'anisotropie des surfaces du matériau, des essais ont été effectués selon trois directions: une longitudinale, correspondant à la direction de laminage de l'échantillon (0°), une transversale, qui représente la direction perpendiculaire à la direction de laminage dans le plan de la plaque (90°) et une direction médiane (45°). Étant donné l'observation de l'anisotropie volumique et surfacique, voir d'une nature fractale de la surface du matériau, des études ont été effectuée afin de déterminer l'influence sur la nature anisotrope des propriétés tribologiques. Les caractéristiques de type fractal du frottement ont été déterminées en utilisant une force normale constante définie par F_n = 7N et en considérant les cinq vitesses de glissements ci-dessus définies.

Abstract:

This scientific paper aims to study the influence of the anisotropy of an aluminium AA2024-T251 rolled thick plate on the surface tribologic properties based on previous experimental and numerical studies concerning bulk and surface mechanical behaviour. Experimental friction tests were made on

a thick plate using an ultra-high-molecular-weight polyethylene (UHMWPE) disk. The used tribometric test involves the generation of local motion along specified trajectories with different orientations under the action of a constant normal force and a constant slip velocity. Three different normal forces (3N, 5N, 7N) have been applied using five different sliding speeds (0.005 mm/s, 0.05 mm/s, 0.5 mm/s, 1mm/s and 5mm/s) along a linear trajectory of 3 mm length. In order to analyze the influence of the aluminium alloy anisotropy, the tests have been performed along three directions: a longitudinal one, corresponding to the rolling direction of the sample (0°), a transverse one, which represents the direction perpendicular to the rolling direction (90°), and a median direction (45°). Taking into account the observed bulk and surface anisotropy, especially concerning a fractal nature of the surface topography, an investigation was performed in order to determine its influence on the anisotropic tribologic properties. In this purpose, fractal friction characteristics have been determined for the sliding process using a constant normal force F_n=7N and the above five sliding speeds.

Keywords: anisotropy, tribology, aluminium alloy, friction fractal analysis

1 Introduction

Friction has an important role in many industrial manufacturing processes and the actual development of numerical engineering design tools requires reliable analyses of friction phenomena and rigorous identification of material's tribologic properties. The application of low weight materials as aluminium alloys and plastics used by the automotive, railways and aeronautics industry has grown since their introduction in the mid-1970s. During the past three decades has been designed a lot of joint metallic-plastics structures, mechanical assemblies and couplings, particularly defined by aluminium alloy-plastic interfaces (Figure 1).

Figure 1. Examples of aluminium alloy-plastics interfaces. (a) Jaw coupling; (b) Telescopic sliding system.

The contact area of these types of materials couples undergoing generally a dry or a boundary lubrication friction, a slow speed sliding and an intermittent moving within tabulated limits of temperature. Many plastics are even self-lubricating, have an extremely corrosive resistance, a high chemically resistance and therefore eliminate the possibility of failures from lack of maintenance. The most commonly used in industry are the phenolics, the acetals, the teflon (PTFE), the ultra high molecular weight polyethylene (UHMWPE) and the nylon [1]. In most sliding or rolling kinetics during material forming processes the friction causes loss energy and high material's wear (forging, extrusion, cutting, etc) and in these cases, friction should be minimized (forging – low friction along the rib). There are a lot of cases where friction has a driving role (rolling – minimal friction requirement, forging – increased friction on the outer flat) or where friction must be optimized (deep drawing, stretch forming process) [2]. It is known today that friction between two solid surfaces is a very complex phenomenon that depends not only on the physical and chemical properties of the materials involved, but also on the thermo-mechanical properties of the contact surfaces. All the study

of friction is mostly based on experimental, theoretical and numerical studies. Depending on the nature of the materials and of the experimental conditions, the general evolution of a friction forces can be presented in Figure 2 [3].

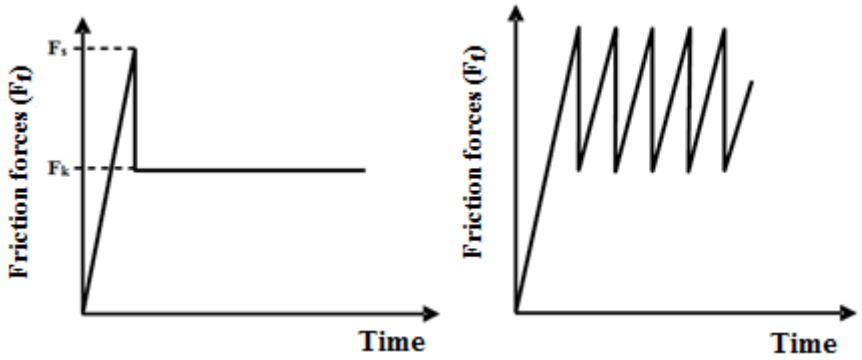

Figure 2. Evolution of the friction force through the time. (a) sliding without stick-slip; (b) stick-slip sliding [3].

Under a normal force F_n, the Coulomb coefficient of static friction μ_s corresponding to $F_f = F_s$ is distinct from the Coulomb coefficient of kinetic friction μ_k corresponding to $F_f = F_k$ as illustrated in Fig.2a. F_s is the maximum force required to have a motion of solid, and F_k is the force applied to maintain this motion [4]:

$$F_s = \mu_s F_n \qquad F_k = \mu_k F_n \tag{1}$$

The classical stick-slip (shown in Fig.2b) requires that the static friction coefficient to be markedly greater than the kinetic friction coefficient. In the case of sliding surfaces, the period of the contact between two points on the two surfaces is longer when the surfaces slide slowly than when they move rapidly. If the sliding of one surface over another slows down, friction increases. This is the situation that favours the stick-slip. The phenomenon appears in metallic friction couples with dry or limited friction regime, when the sliding speed is in the range of 0.01 – 3 mm/s or when the angular speed is somewhere in the 1 – 25 rad/s range. Studies of sliding at slow speeds are important because they lead systematic information of friction-velocity relations, which will enable for the engineering designers to select materials that will not be affected by stick-slip phenomenon. There are three main classical methods to conserve or reduce stick-slip phenomenon: changing the sliding speed (in some cases slowing down, in some cases speeding up), reducing the stored energy or to lubricate the sliding surfaces [5, 6]. The main purpose of this work is to analyze the rheological and tribological behaviour especially regarding the influence of the anisotropic properties on the metallic-plastic interfaces.

2 Anisotropic Material Properties

Aluminium alloys are widely used in many industrial fields such as aeronautics, naval, railway and automotive. The most considerable particularities of aluminium alloys are their good ductility (especially at high temperatures), high electrical conductivity, low specific weight and their very good formability and workability. Because of these excellent thermo-mechanical and physical characteristics, the usage of aluminium has an ever-increasing importance in a large lot of industrial manufacturing industry: rolling, extrusion, molding, embossing, stamping and welding [7]. This paper proposes to analyze bulk and surface anisotropic properties of the aluminium alloy AA2024-T351 rolled thick plate (thickness = 10 mm). The main mechanical properties of this aluminium alloy are defined by an ultimate tensile strength higher than 420 MPa, a HD harshness around 120 Kgf/mm^2 and a yield strength 0.2%>260 MPa. Experimental and the numerical identified anisotropic elasto-plastic parameters are shown in the Table 1 and the Table 2, starting from previous experimental, theoretical

and numerical works [9-11]concerning the bulk plastic anisotropic behaviour conducted at GCGM laboratory of National Institute of Applied Sciences of Rennes.

Table 1. Elasto-plastic parameters of the anisotropic aluminium alloy AA2024-T351 [9-11].

Elasticity Parameters		Yield Stress [MPa] ($\bar{\varepsilon}^p$=0.2%)			Voce Law (0°) $\sigma(0°)=\sigma_0(0°)+\mathrm{K}\left[1-\exp(-n\bar{\varepsilon}^p)\right]$		Lankford coefficients ($\bar{\varepsilon}^p$=0.2%)		
E [MPa]	υ	σ_0(0°)	σ_0(45°)	σ_0(90°)	K [MPa]	n	r_0	r_{45}	r_{90}
72653	0.33	301.	266.	250.	250.	18.	0.61	0.73	0.59

Table 2. Experimental and numerical identified Hill's 1948 coefficients of AA2024-T351 [9-11].

Hill Parameters (MPa)	F	G	H	L = M = N
Experimental Plane Anisotropy ($\bar{\varepsilon}^p$=0.2%)	0.64	0.62	0.38	1.74
Experimental Normal Anisotropy ($\bar{\varepsilon}^p$=0.2%)	0.60	0.60	0.40	1.40
Numerical Identification of Plane Anisotropy	0.50	0.63	0.37	0.97
Numerical Identification of Normal Anisotropy	0.63	0.63	0.36	1.35

In the case of a rolled sheet an orthotropic plastic anisotropy is generally assumed considering three specific material orientations: x-rolling direction LD (0°), y-transverse direction TD (90°) and z-thickness direction. The plane and the normal anisotropy are analyzed from the estimation of the Lankford coefficient *r* which represents the ratio between the transversal plastic strain rate and the thickness plastic strain rate. Experimental tensile tests have been realized using 0°, 45° and 90° load orientations with respect to the rolling direction for a lot of specific AA20124-T351 specimens with 3 mm thickness. The experimental values of Lankford coefficients r_0, r_{45}, r_{90} have been computed from measurements of local longitudinal and transversal plastic strain rate corresponding to 12% equivalent plastic strain (Table 1). According to the Lankford analysis, dimensionless coefficients of the following Hill'48 yield criterion are also computed using specific hypothesis (Table 2).

$$\Phi([\sigma]) = F(\sigma_{yy}-\sigma_{zz})^2 + G(\sigma_{zz}-\sigma_{xx})^2 + H(\sigma_{xx}-\sigma_{yy})^2 + 2L\tau_{yz}^2 + 2M\tau_{zx}^2 + 2N\tau_{xy}^2 - \sigma^2(0°) = 0 \quad (1)$$

For a plane anisotropy model (generally used to describe anisotropy of thin sheets) if a reference equivalent stress along 0° direction is considered $G + H = 1$ and consequently only three independent Hill parameters *F*, *G* and *N* can be computed using specific relationships expressed in terms of Lankford coefficients [11]. For a thick plate a general orthotropic three-dimensional plastic anisotropy must be defined. In a first approximation if the experimental planar anisotropy coefficient $\Delta\bar{r} \approx 0$ (here $\Delta\bar{r} = -0.06$) a normal anisotropy can be used. In this case $F = G$ and $N = F + 2H$ where the shear anisotropic parameters *L* and *M* are keep equal to *N* i.e. $L = M = N$. The Hill parameters were also identified numerically by finite element simulations [10-11] starting from an interactive-graphic non-linear regression of the stress-plastic strain curves obtained from tensile tests along 0°, 45° and 90°. A Voce hardening law has been used to define a reference equivalent stress using the tensile curve obtained from 0° orientation. These identified anisotropic Hill criterion permits to describe the bulk mechanical behaviour and the macroscopic surface stress state of elasto-plastic contact interfaces.

3 Experimental Tribological Procedure

For this study a tribological analysis of the aluminium alloy AA2024-T351 rolled thick plate (thickness = 10 mm) has been performed with a pion-plan tribometer by using an ultra-high-

molecular-weight polyethylene (UHMWPE) disk. This polymer is characterized by an excellent resistance to abrasion and its main mechanical properties: ultimate tensile strength around 38.6-48.3 MPa, yield strength of 21.4-27.6 MPa, Young's modulus E = 894-963MPa and Poisson's coefficient of 0.46 [8]. The experimental UMT Tribometer (OMT Department of UPB) is presented in the Figure 2. This tribometer can provide rotational, translational or reciprocal motions with speeds starting from 0.1µm/s up to 10m/s. A constant or progressive load between 0.05 N and 1000 N can be applied on the sample surface [12]. In order to analyze the influence of the bulk and surface material anisotropy, the tribological tests were made on three directions (Fig. 3): a longitudinal one LD (0º), corresponding to the rolling direction of the sample, a transversal one TD (90°) which represents the direction perpendicular to the rolling direction and a median direction DD (45º).

Figure 3. UMT Tribometer.

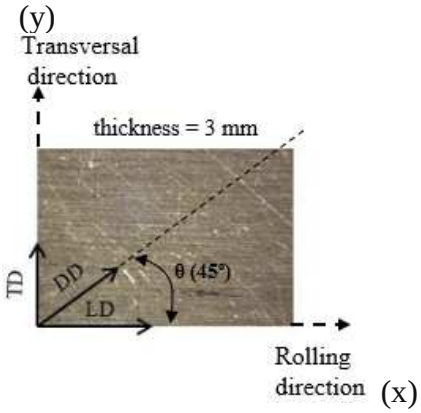

Figure 4. Measuring directions (rolled AA2024-T351 plate).

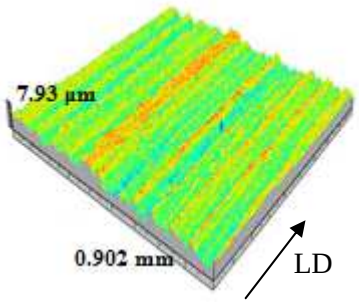

Figure 5. 3D Optical surface profilometry.

The test involves moving a polyethylene disk along a specified trajectory under a constant normal force and at a constant speed (Fig. 4). All the tribological tests were performed with three different forces (3N, 5N, 7N) and five different speeds (0.005 mm/s, 0.05 mm/s, 0.5 mm/s, 1mm/s, 5mm/s) along a linear trajectory with a length around 3 mm.

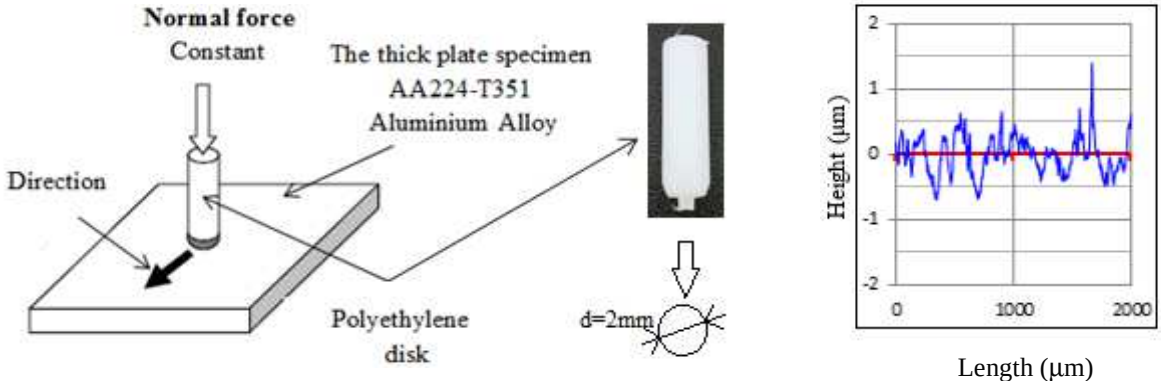

(a) (b)

Figure 6. Friction test conditions. (a) Tribometer schema; (b) Surface micro-topography.

Starting from previous works of authors [13-14] where micro-topography of the rolled aluminium alloy AA2024-T351 surface was studied, the random nature of the roughness height was described through statistical and fractal analysis. Roughness is one of the main characteristics of surface quality and it can be determined by non-contact measurement methods such as optical scanning of the surface shape (Fig.5) and by special contact profilometers (Fig. 6b). A specific roughness structural function method was used to compute the corresponding fractal dimension D_f. It was observed that the samples surface have fractal behaviour up to 1.1 µm. The estimated values of D_f and the corresponding variation curves have shown that the effect of the fractal dimension are smaller for the longitudinal direction and they have similar values for transversal and diagonal directions.

4 Anisotropic Friction Analysis

The time variation of the tangential forces F_f for all measurements corresponding to three normal forces F_n (3N, 5N, 7N) and five different sliding speeds v_g are presented in Fig.7.

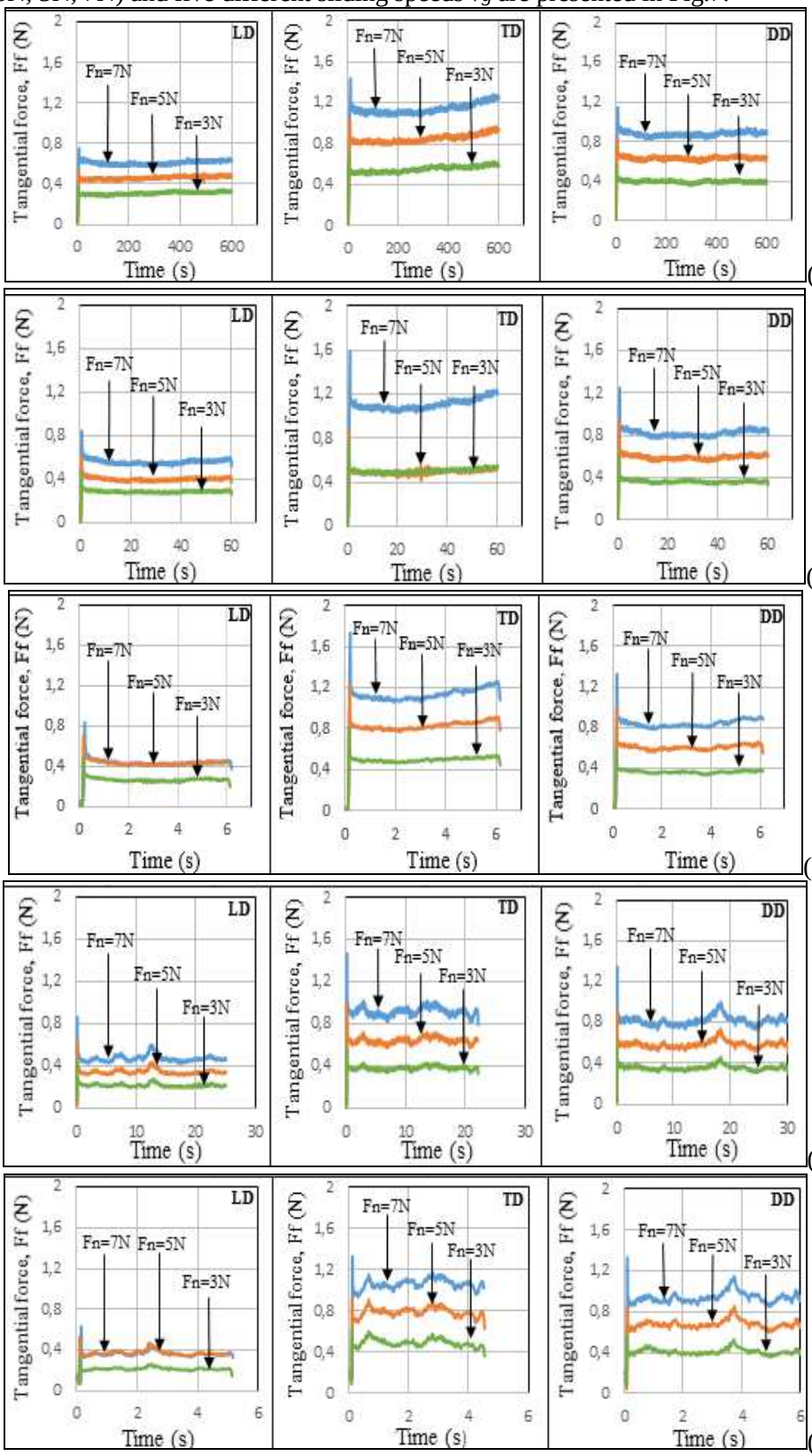

Figure 7. The time variation of the tangential force for the longitudinal (LD), transversal (TD) and median (DD) directions. (a) 0.005mm/s; (b) 0.05mm/s; (c) 0.5mm/s; (d) 1mm/s; (e) 5mm/s.

Because of the polyethylene semi-crystalline nature, which has excellent abrasion resistance and good sliding properties, it is observed that the evolution of the friction forces through time reveals a sliding without stick-slip with a relatively steady state, even for low and moderate speeds. As can be seen from the pictured results in Figure 7, the kinetic tangential force has values between 0.1-0.7N for the longitudinal direction (0º), between 0.5-1.2N for the transversal direction (90º) and between 0.4-0.8N for the median direction (45º). It can be seen that there is a similarity between the friction forces corresponding to the transversal and the median sliding directions. The Table 3 synthesises the static and kinetic Coulomb friction coefficients estimated by the ratio of the F_f and F_n along the three surface specimen directions: rolling or longitudinal (LD), transversal (TD) and median (DD) directions.

Table 3. The average values of Coulomb static and kinetic friction coefficient (p_c - contact pressure).

Normal force F_n [N]	Sliding speed v_g [mm/s]	Coulomb static friction coefficient (μ_s)			Coulomb kinetic friction coefficient (μ_k)		
		LD	TD	DD	LD	TD	DD
7 (p_c = 2.22 MPa)	0.005	0.107	0.205	0.164	0.086	0.162	0.125
	0.05	0.120	0.224	0.177	0.080	0.158	0.116
	0.5	0.165	0.242	0.185	0.086	0.162	0.119
	1	0.122	0.209	0.190	0.066	0.130	0.116
	5	0.126	0.186	0.189	0.072	0.138	0.123
5 (p_c = 1.59 MPa)	0.005	0.106	0.205	0.165	0.092	0.170	0.126
	0.05	0.123	0.284	0.184	0.080	0.165	0.118
	0.5	0.140	0.242	0.193	0.086	0.164	0.121
	1	0.126	0.198	0.185	0.068	0.128	0.117
	5	0.104	0.181	0.170	0.073	0.143	0.124
3 (p_c = 0.95 MPa)	0.005	0.123	0.228	0.191	0.102	0.184	0.132
	0.05	0.152	0.257	0.202	0.096	0.167	0.120
	0.5	0.161	0.259	0.120	0.089	0.163	0.122
	1	0.142	0.273	0.198	0.070	0.126	0.118
	5	0.111	0.205	0.189	0.071	0.148	0.126
Mean values		0.133	0.238	0.176	0.089	0.166	0.122

It can be observed that the sliding direction (longitudinal, transversal or median) influences the tangential forces F_f and the friction coefficients. The highest values occur for the direction orthogonal to the rolling direction (TD) and the lowest for the coefficient in the rolling direction (LD). So regarding the mean values of Coulomb coefficients these ones are around of 80% higher along the TD direction as compared to those of LD direction. These results confirm the higher influence of the sliding stretching along the direction orthogonal to the longitudinal distribution of the surface asperities (Figure 5). It is then necessary to define anisotropic friction law. Based on plastic theory applied to description of metallic materials behaviour similar friction criteria can be defined using maximal work principle and normal rule of convex surface friction loci [15]. Regarding the plastic anisotropic Hill formulation (1) used to describe bulk anisotropic behaviour of AA2024-T351 aluminium alloy, in a similar way the following quadratic elliptic friction criterion Ψ is chosen:

$$\Psi(\vec{\tau}) = \Psi(\tau_x, \tau_y) = G_f \tau_x^2 + H_f \tau_y^2 - \lambda^2 = 0 \tag{2}$$

Here τ_x, τ_y represent the axis components of surface tangential stress $\vec{\tau} = \tau_x \vec{x} + \tau_y \vec{y}$ along the orthotropic plate axis *x* (LD direction) and *y* (TD direction). Taking into account the orientation angle α of friction shear stress $\vec{\tau}$ the corresponding two components along the orthotropic surface axis are defined by

$\tau_x = \tau\cos(\alpha)$ and $\tau_y = \tau\sin(\alpha)$. Because the sliding direction $\vec{n}_g$ defined in the *xy* plane by an angle θ is obtained from the normal of the convex friction criterion i.e. $\vec{n}_g = -\vec{v}_g / \|\vec{v}_g\| = (\partial\Psi/\partial\vec{\tau})(\|\partial\Psi/\partial\vec{\tau}\|)$ it can be shown that $tg(\theta) = (H_f / G_f)\,tg(\alpha)$, $\tau(\alpha) = \mu_f(\alpha)p_c = \mu_f(\theta)p_c$ and $\mu_f(\theta) = \sqrt{(\cos^2(\theta)/G_f) + (\sin^2(\theta)/H_f)}$. According to the friction values obtained for θ = 0° (LD with α = 0°) and θ = 90° (TD with α = 90°) and taking into account the local Coulomb friction law with $\tau(0°) = \mu_f(0°)p_c$ and $\tau(90°) = \mu_f(90°)p_c$ it is easy to verify from (2) that $G_f = 1/\mu_f^2(0°)$, $H_f = 1/\mu_f^2(90°)$ and $\lambda = p_c$. Consequently the anisotropic friction law can be written by:

$$(\tau_x^2/\mu_f^2(0°)) + (\tau_y^2/\mu_f^2(90°)) = p_c^2 \text{ with } \mu_f(\theta) = \sqrt{\mu_f^2(0°)\cos^2(\theta) + \mu_f^2(90°)\sin^2(\theta)} \quad (3)$$

Regarding the mean values of contact pressure (p_C = 1.58 MPa) and of frictions coefficients from Table 3, in the case of the sliding along the median direction DD (θ = 45°) the corresponding friction coefficients have a magnitude close to the root mean square of LD and TD values (0.193 for static friction and 0.133 for kinetic friction, respectively 9%-9.5% error estimation) with a shear stress orientation $\alpha \approx 60°$ (Figure 8).

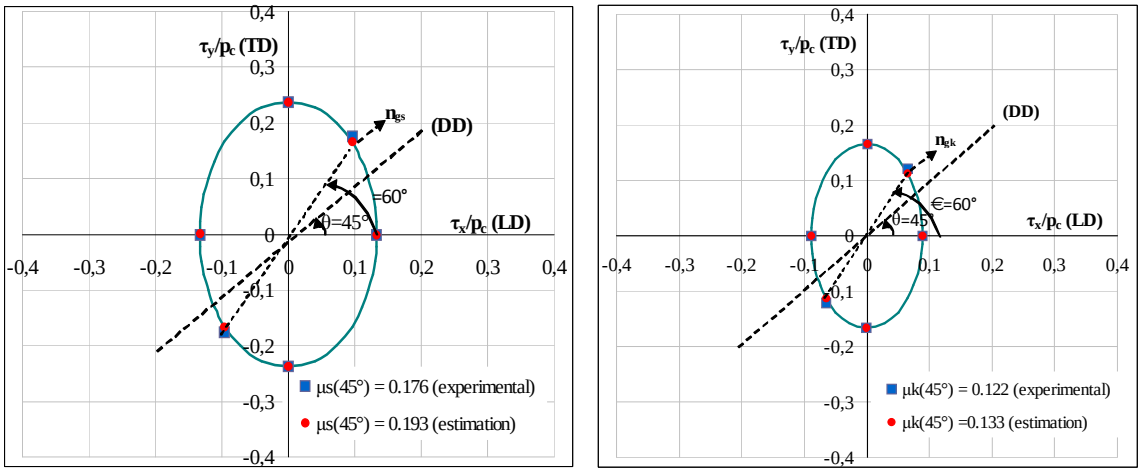

(a) (b)

Figure 8. Elliptic anisotropic friction criterion concerning rolled AA2024-T351/UHMWPE polyethylene sliding contact; a) static friction; b) kinetic friction.

Consequently the above expression (3) describes with a good approximation the observed anisotropic surface friction. Concerning the sliding velocities and the contact pressures these mechanical contact variables have relatively small influences (10%-15%) on the estimated friction coefficients. A weak maximum peak is reached especially for a sliding speed of 0.5 mm/s.

5 Tribological Fractal Analysis

Surface roughness has a large impact on the tribological phenomena such as contact mechanics, friction, wear, lubrication, etc. When two flat surfaces are in contact, surface topography causes discrete contact points. The mode of surface deformation may be elastic, elastic-plastic or plastic and depends on surface topography, mechanical and physical material proprieties, normal and shear forces or stresses. Fractal geometry method has been widely used in recent years and can be applied to characterize surface topography and contacts mechanics [16,17]. According to the previous work of authors concerning fractal surface geometry analysis of the anisotropic AA2024-T351 plate [13], the

purpose of the study is to investigate the fractal character of the friction coefficient evolution during the transition between the static state and the kinetic one in the case of a sliding process between a polyethylene disk and the rolled AA2024-T351 surface plate. It is then proposed to analyse the friction curves of the Figure 7 corresponding to the higher contact pressure p_c = 2.22 MPa (constant normal force F_n = 7N) and the chosen constant five speeds. The fractal dimension of friction coefficient variation $D\mu$ can be computed using the following equations [16,17]**:**

$$D\mu = \frac{4 - D_s}{2}, \quad 0 < D_s < 2 \tag{4}$$

The slope of this function D_s, plotted on double logarithmic coordinates, is estimated by using three points defined by $x_{fs} = \{x_{fs1}, x_{fs2}, x_{fs3}\}$, $y_{fs} = \{y_{fs1}, y_{fs2}, y_{fs3}\}$ of the structure function:

$$D_s = slope\left(x_{fs}, y_{fs}\right) \tag{5}$$

The slope is a measure of the steepness of a line, or a section of a line, connecting two points and is computed by finding the ratio m of the "vertical change" to the "horizontal change" between (any) two distinct points on a line i.e. $m = \Delta y / \Delta x$. The friction structure function $S\mu$ can be written as [17-19]:

$$S\mu(N,k) = \frac{1}{N-k}\sum_{i=1}^{N-k}(y_{i+k} - y_i)^2 \tag{6}$$

Here k is the increment of x ordinate, $k = 1…N\text{-}1$ and N is the length of the y vector; here N = 2000, except the tests for 0.5 mm/s where N = 500 and 1 mm/s where N = 400. The straight line that approximates the structure function $S\mu$ can be determined in function of x_f = 0,0.01,...,2. as following:

$$y_f\left(x_f\right) = D_s \cdot x_f + y_{fs1} - D_s \cdot x_{fs1} \tag{7}$$

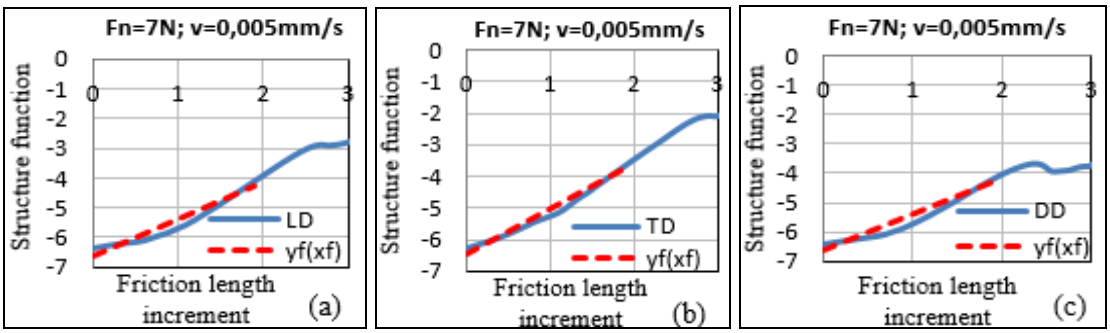

Figure 9. Log-Log curves (structure function-correlation length) and the straight line ($y_f(x_f)$) for F_n=7N and v=0.005mm/s; (a) longitudinal direction (LD); (b) transversal direction (TD); (c) median direction (DD).

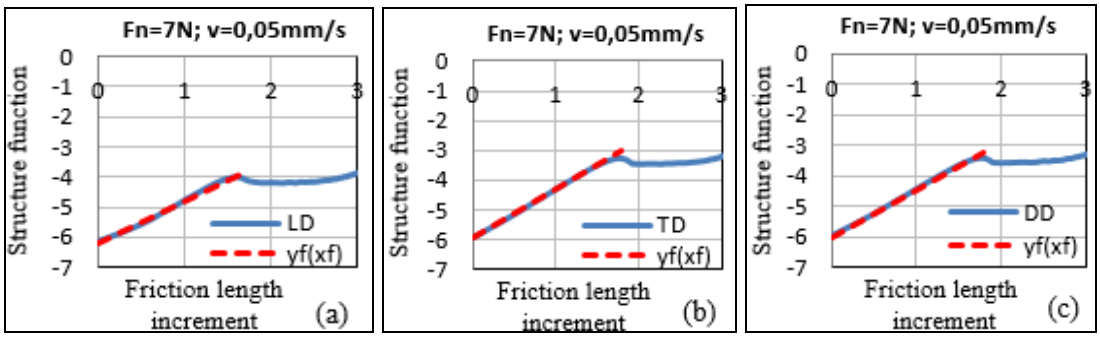

Figure 10. Log-Log curves (structure function-correlation length) and the straight line ($y_f(x_f)$) for F_n=7N and v=0.05mm/s; (a) longitudinal direction (LD); (b) transversal direction (TD); (c) median direction (DD).

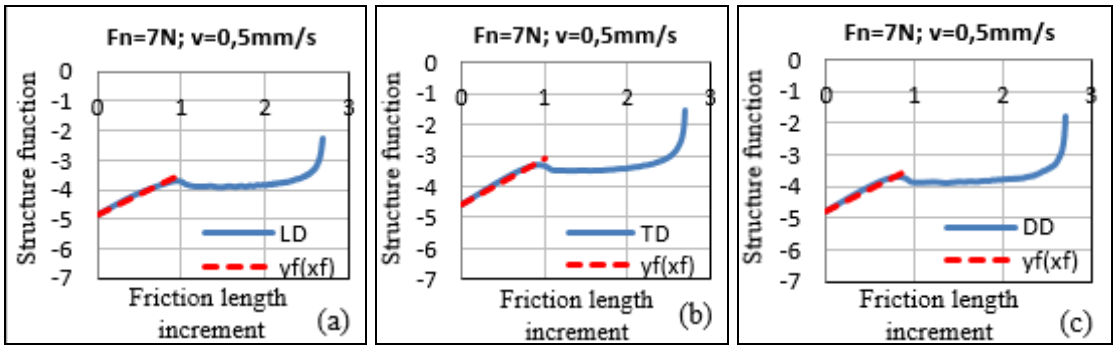

Figure 11. Log-Log curves (structure function-correlation length) and the straight line ($y_f(x_f)$) for F_n=7N and v=0.5mm/s; (a) longitudinal direction (LD); (b) transversal direction (TD); (c) median direction (DD).

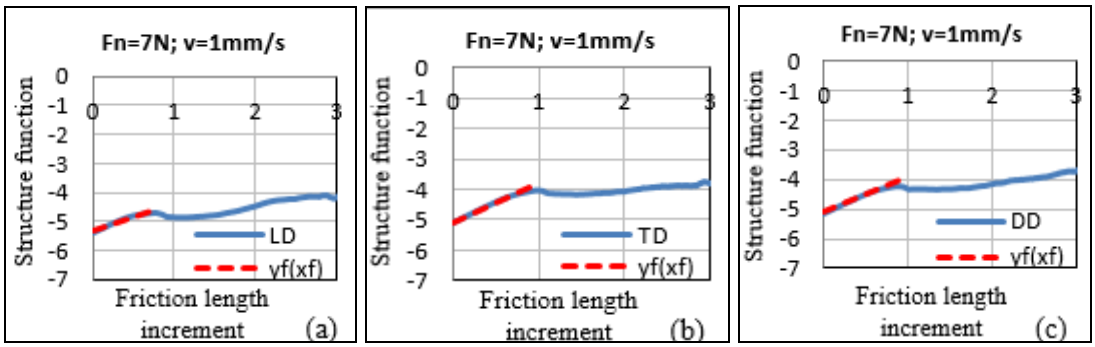

Figure 12. Log-Log curves (structure function-correlation length) and the straight line ($y_f(x_f)$) for F_n=7N and v=1mm/s; (a) longitudinal direction (LD); (b) transversal direction (TD) ; (c) median direction (DD).

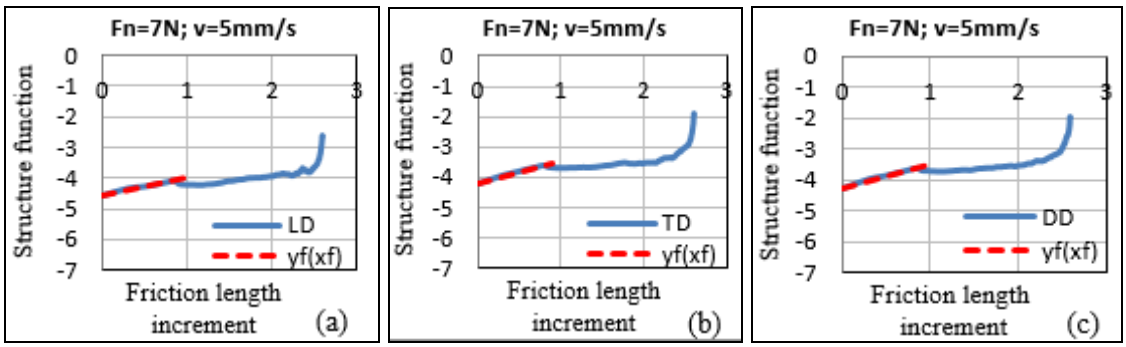

Figure 13. Log-Log curves (structure function-correlation length) and the straight line ($y_f(x_f)$) for F_n=7N and v=5mm/s; (a) longitudinal direction (LD); (b) transversal direction (TD); (c) median direction (DD).

The figures 9-13 describe the log-log curves (friction structure function - correlation length) and the corresponding straight line ($y_f(x_f)$, where ($y_f = log(S\mu(N,k)$ and $x_f = log(k)$) that approximates the friction structure function variation of measurements along the three directions (LD, TD and DD). From the plotted log-log curves and the corresponding straight line ($y_f(x_f)$) it can be observed that the friction coefficient evolution, especially during the transition between static and kinetic sliding, reveals a fractal character up to 20 time's increment point (around a sliding distance of 0.025 mm) for v=0.5mm/s, v=1mm/s,v=5mm/s and up to 80 time's increment point (around a sliding distance of 0.150 mm) for v=0.05mm/s. For the lowest speed (v=0.005mm/s) the friction coefficient variation doesn't have a fractal character (*). The computed values of the friction fractal dimension D_μ for all

measurements are presented in Table 4 and Table 5.

Table 4. The friction fractal dimension values for v=0.005mm/s, v=0.05mm/s and v=0.5mm/s *(F_n=7N)*.

Friction Fractal Dimension $D\mu$								
F_n=7N; v=0.005mm/s			**F_n=7N; v=0.05mm/s**			**F_n=7N; v=0.5mm/s**		
LD	TD	DD	LD	TD	DD	LD	TD	DD
*	*	*	1.305	1.202	1.226	1.384	1.284	1.393

Table 5. The friction fractal dimension values for v=1mm/s, v=5mm/s (*F_n=7N)*.

Fiction Fractal Dimension $D\mu$					
F_n=7N; v=1mm/s			**F_n=7N; v=5mm/s**		
LD	TD	DD	LD	TD	DD
1.526	1.346	1.406	1.716	1.623	1.605

It can be shown that the computed friction fractal dimension is increasing with the speed and have relatively similar values for TD and DD directions. The higher values are obtained for sliding along the rolling direction LD. All these friction fractal information show that concerning the measuring of a steady state kinetic friction it can be used measurements values of tangential forces for a distance sliding between 0.025 mm and 0.150 mm. Furthermore the computed friction fractal dimension $D\mu$ can be used to estimate an average ratio between the static friction coefficient and the kinetics one.

6 Conclusions

The main purpose of this scientific study was to determine the influence of material anisotropy on the sliding of an ultra-high-molecular-weight polyethylene (UHMWPE) disk over a rolled aluminium alloy AA2024-T351 plate in the range of low and moderate sliding speeds. Starting from previous works rheological elastic and plastic parameters of an anisotropic plastic Hill criterion has presented to describe and understand the bulk anisotropy of studied aluminium rolled plate. To characterise surface friction properties a lot of tribologic tests have been performed using the movement of a polyethylene disk along a linear trajectory (3mm) under a constant normal force (three different forces: 3N, 5N, 7N) and at constant sliding speeds (0.005 mm/s, 0.05 mm/s, 0.5 mm/s, 1mm/s, 5mm/s). All the experimental tests were made along three directions: a longitudinal one (LD or 0º), corresponding to the rolling direction of the sample, a transversal one (TD or 90º), which represents the direction perpendicular to the rolling direction and a median direction (DD or 45º). According to the obtained results it can be concluded that the rolling AA2024-T351 thick plate has anisotropic tribologic properties. So the sliding direction influences the friction coefficient: the lowest coefficient occurs for the longitudinal direction, the highest for the transversal direction and a root square mean value for the median direction. It has been also observed that Coulomb coefficients have a relatively small variation with the sliding speeds and contact pressure and reaching maximum values generally for a sliding speed of 0.5 mm/s. A quadratic elliptic function has been identified to describe the observed anisotropic surface friction with an average error around of 10%. Furthermore the variation of the friction force or of the Coulomb friction coefficient versus time does not describe a stick-slip sliding generally characterising small and very small sliding speeds due to the nature of polyethylene surface properties. Concerning the analysis of the transitions between the static friction and the steady sliding state, the investigation of the friction coefficient evolution reveals a fractal character. The log-log curves (friction structure function-correlation length), the straight line ($y_f(x_f)$) and the fractal dimension shows a friction fractal character up to 0.025 mm – 0.150 mm sliding distance, except for the very small sliding speed (0.005 mm/s). Differences of fractal friction dimensions along the three

orthotropic material directions confirm the anisotropic tribologic properties observed by the material surface topography and Coulomb friction coefficients estimation.

References

[1] E. Gustafsson, Investigation of friction between plastic parts, Master Thesis, Chalmers University of Technology, Göteborg, Sweden 2013.
[2] P. Menezes, S. Ingole, M. Nosonovsky, S. Kailas, M. Lovell, Tribology for Scientists and Engineers, From Basics to Advanced Concepts, Springer (2013), pp. 43-44.
[3] R. P. Nachane, G. F. S Haussain, K. R. Krishana Iyer, Theory of the stick-slip effect in friction, Indian Journal of Fibre & Textile Research 23 (1998), pp. 201-208.
[4] J. Takadoum, Materials and Surface Engineering in Tribology, first published by Hermes Science/Lavoisier entitles: "Matériaux et surfaces en tribologie", Paris, France, 2007, pp. 63-64.
[5] N. A. Stoica, A. Tudor, Some Aspects Concerning the Behaviour of Friction Materials at Low and Very Low Sliding Speeds, Tribology in Industry 37 (2015), pp. 374-379.
[6] S. S. Antoniu, A. Cameron, The friction-speed relation for stick data, Wear 36(1976), pp. 235-254.
[7] E. Cazimitrovici, M.V. Suciu, Laminarea Materialelor Metalice Speciale, Editura BREN, Bucharest, Romania, 2000.
[8]Generic Material Properties of Ultra High Molecular Weight Polyethylene (UHMWPE). http://www.dielectriccorp.com/downloads/thermoplastics/uhmw.pdf
[9] E. Pirva, Etudes mécaniques et multi-échelle du comportement isotrope et anisotrope 3D en grandes déformations plastiques. Application à la modélisation numérique de l'emboutissage profonde des tôles des alliages d'aluminium, Master Thesis, Supervisor: A. Gavrus, INSA Rennes, France, 2014.
[10] W. Nasri, A. Gavrus, A. Kouadri-David, K. Sai, Applications of multi-scale models to numerical simulation and experimental analysis of anisotropic elastoplastic behavior of metallic sheets, Key Eng. Mat. 611-612 (2014), pp. 536-544.
[11] W. Nasri, A. Gavrus, A. Kouadri-David, K. Sai, Experimental characterization and numerical modeling of three-dimensional anisotropic behavior of a thick sheet aluminum alloy AA2024-T351 using multi-scale approaches, WIT Transactions on The Build Environment 166 (2016), pp. 163-177.
[12] UMT Multi-Specimen Test System Hardware Installation & Applications Manual
Available at http://erc.ncat.edu/Facilities/Manuals/CETR_UMT2_Manual.pdf
[13] E Pirva, A Tudor, A Gavrus, Fractal analysis of surface micro-topography for a rolled anisotropic thick sheet of aluminium alloy (AA2024-T351), IOP Conference Series: Materials Science and Engineering 147 (2016).
[14] E. Pirva, A. Tudor, A. Gavrus, G. Chisiu, N. Stoica, A. Predescu, Micro-scratching tests of a rolled aluminium alloy AA2024-T351 thick plate using a diamond micro-blade, IOP Conference Series: Materials Science and Engineering 174 (2016).
[15] P. Montmitonnet, F. Delamare, E. Feldre, N. Marsault, Cours de Tribologie de la Mise en Forme, Master/DEA, Ed. Ecole Nationale des Mines de Paris, France, 1992.
[16] H. Zahouani, R. Vargiolu, J.L. Loubet, Fractal Models of Surface Topography and Contact Mechanics, Mathl. Comput. ModelIing 28 (1998), pp. 517-534.
[17] B. Bhushan, Contact mechanics of rough surfaces in tribology: Single asperity contact, Appl Mech Rev 49 (1996) pp. 275-297.
[18] Y. Morag, I. Etsion, Resolving the contradiction of asperities plastic to elastic mode transition in current contact models of fractal rough surfaces, Wear 262 (2007), pp. 624-629.
[19] B. B. Mandelbrot, The fractal geometry of nature, Phys. Scr. (1982), pp. 257-260.